CONF-8605150--3

CONF-8605150--3

DE87 005498

Proceedings of Beijing International Symposium on Physics at Tandem, May, 1986.
Beijing, China

HIGH-SPIN STATES AND COEXISTING STATES IN THE Pt-Au TRANSITION REGION

L. L. Riedinger, M. P. Carpenter, L. H. Courtney, V. P. Janzen, and W. Schmitz

University of Tennessee, Knoxville, TN 37996-1200, USA

AS05-76ER04936

Abstract: High-spin states in the N = 104 to 108 region have been studied by in-beam spectroscopy techniques in a number of Ir, Pt, and Au nuclei. These measurements have been performed at tandem Van de Graaff facilities at the Oak Ridge National Laboratory and at McMaster University. Through comparison of band crossings in a variety of odd-A and even-A nuclei, we are able to assign the first neutron and first proton alignment processes, which are nearly degenerate for ^{184}Pt. These measurements yield the trend of these crossing frequencies with N and Z in this region. Knowledge of this trend is important, since these crossing frequencies can give an estimate of how the shape parameters vary across this transitional region.

The spectroscopy of nuclear states in a transition region has been an important way of studying the effects of varying shape parameters on the nuclear observables. Much work has been performed in the N = 90 region, where one observes the onset of prolate shapes and thus rotational spectra as a function of neutron number. The transitional nuclei at the end of the rare-earth deformed region have been less completely studied but offer more challenges to nuclear models by virtue of more degrees of freedom. Unlike the N = 90 nuclei, those in the N = 106 region exhibit not only a gradual transition from prolate to spherical excitations but also states built on oblate configurations. Effects observed in the light Pt and Au nuclei appear to be suggestive of larger variations in the shape parameters than in the light rare-earth nuclei and thus allow us to test our models in a stringent manner. Measurements by our group and others give rise to the co-existence of prolate and oblate states at low spins. One result of this work has been to demonstrate that collective models based on Woods-Saxon or Nilsson potentials can indeed explain the gross features of both these co-existing states and also the band crossings which occur at higher spins.

The first step toward the understanding of high-spin states in the N = 106 region is to observe the band crossings which occur at moderate rotational frequencies. It has been clear for some 15 years that band crossings or backbends are the major events which affect the nucleus in its rotational modes. The observable parameters of these band crossings (rotational frequency of the crossing, alignment gain, interaction strength) can be calculated in various phenomenological models. These measured characteristics of the backbends in any region of nuclei can then be used as an indirect measure of the field parameters used in the calculations. This is especially important in the N = 106 transition region, where the shape parameters are expected to vary widely due to the close lying nature of prolate and oblate states. Our measurements on bands in ten different nuclei in this region establish the systematic trend of the first neutron and proton alignment processes in light Ir, Pt, and Au nuclei. Comparison of these measured fingerprints of the crossings to the results of self-consistent cranked HFB calculations [1,2] gives us an initial understanding of the variation of the shape parameters across this transition region.

Our group has been involved in a series of measurements of rotational bands in a number of different nuclei using arrays of gamma-ray detectors and heavy-ion induced reactions. These results are rather pertinent to this Beijing conference since all experiments were performed with tandem Van de Graaff accelerators, either the large 20-MV machine at Oak Ridge or the 11-MV FN device at McMaster University. The experiments performed on the various nuclei are listed in Table 1.

These experiments have been performed with a large multiplicity

Table 1. Experiments performed and group with major analysis responsibility.

Final Product	Reaction	Beam Energy	Accel.	No.Ge Detect.	Multiplicity Filter	Major Group
^{185}Pt	^{34}S,5n	163 MeV	HHIRF	8[1]	SS[2]	Stockholm/UT
^{184}Pt	^{34}S,4n	163	HHIRF	8	SS	UT
^{183}Au	^{35}Cl,4n	170	HHIRF	11	SS	UT
^{185}Au	^{19}F,4n	97	McMaster	5	6 NaI	UT
^{186}Au	^{19}F,4n	94	McMaster	5	6 NaI	UT
^{187}Au	^{19}F,4n	95	McMaster	5	6 NaI	McMaster
^{188}Au	^{19}F,4n	93	McMaster	5	6 NaI	UT
^{187}Pt	^{16}O,4n	95	McMaster	8	6 NaI	McMaster
^{184}Pt	^{16}O,4n	91	McMaster	8	6 NaI	UT
^{185}Pt	^{16}O,4n	90	McMaster	8	6 NaI	Montreal
^{186}Pt	^{16}O,4n	90	McMaster	8	6 NaI	Montreal
^{187}Pt	^{16}O,4n	83	McMaster	8	6 NaI	Montreal
^{188}Pt	^{16}O,4n	85	McMaster	8	6 NaI	McMaster
^{185}Ir	^{19}F,4n	95	McMaster	8	6 NaI	UT

1. In the Holifield experiments, some of the Ge counters were Compton suppressed.
2. SS stands for the Spin Spectrometer, which is an array of 71 NaI counters, some number of which is replaced by Ge detectors.

of collaborators due the complexity of the measurements and the volume of the data. The collaborators and the groups are listed in Table 2, while the group with the major responsibility for the analysis of a particular set of data is shown in Table 1.

Table 2. Collaborators in the various measurements.

Univ. Tennessee	McMaster Univ	ORNL	Univ. Montreal	Res. Inst. Physics	Theory Collab.
C.R. Bingham	J. Johansson	C. Baktash	J. Dubuc	A. Johnson	R. Bengtsson
M.P. Carpenter	G. Kajrys	M.L. Halbert	P. Larivière	J. Nyberg	T. Bengtsson
L.H. Courtney	D. Pogescu	N.R. Johnson	S. Monaro		G. Leander
W.P. Jonzen	J.C. Waddington	I.Y. Lee	S. Pilotte		W. Nazarewicz
A.J. Larabee		M.N. Rao			J.Y. Zhang
Z.M. Liu					
L.L. Riedinger					
W. Schmitz					

The first measurement performed in this series was that on ^{185}Au [3]. The level scheme resulting from this experiment is shown in Fig. 1. The lower spin members of bands 1, 2, and 4 had been observed previously both by our group [4] and that at Grenoble [5]. These three, in addition to band 3, are interpreted as proton excitations built on prolate shapes, bands 1 and 2 due to the "$h_{9/2}$" 1/2[541] Nilsson state, band 3 due to "$f_{7/2}$" 1/2[530], and band 4 from $i_{13/2}$ 1/2[660]. The $11/2^-$ state at 220 keV is a 26 ns isomer [6] and has been assigned as the $h_{11/2}$ state built on an oblate shape (the shape difference explaining the isomerism). The family of high-spin states built on this $11/2^-$ level is seen in Fig. 1 to be representative of both an aligned and a strongly-coupled sequence. The former is interpreted as the coupling of the $h_{11/2}$ single particle excitation to the oblate minimum, the latter to the prolate minimum. This interpretation is reinforced by the calculation of Nazarewicz [7] which shows two such $h_{11/2}$ bandheads lying within 100 keV of each other [2]. Of course, the multitude of transitions between these two structures is indicative of the mixing of their wave functions in the crossing region. A recent UNISOR measurement of the radioactive decay of ^{185}Hg [8] indicates a second $9/2^-$ state which is 313 keV above the $h_{9/2}$ bandhead and decays to it by a transition containing a significant E0 admixture. This seems to be indicative of the $h_{9/2}$ single-particle excitation coupled to near-lying prolate and oblate minima. The prolate minimum is lower here than the oblate since the $h_{9/2}$ excitation is a particle state coupled to a Pt core, where the ground state seems to be prolate [9,10]. In contrast, the $h_{11/2}$ family exhibits the oblate state at a lower energy, since these are hole states coupled to Hg cores where the oblate minimum is lower in energy [11]. It is clear that this $N = 106$ Au nucleus is right at the crossroads of changing prolate and oblate potential minima, the case where the shapes are most energy degenerate. It is in this region that we have studied bands at high angular momenta in order to learn what effect this might have on the high-spin states.

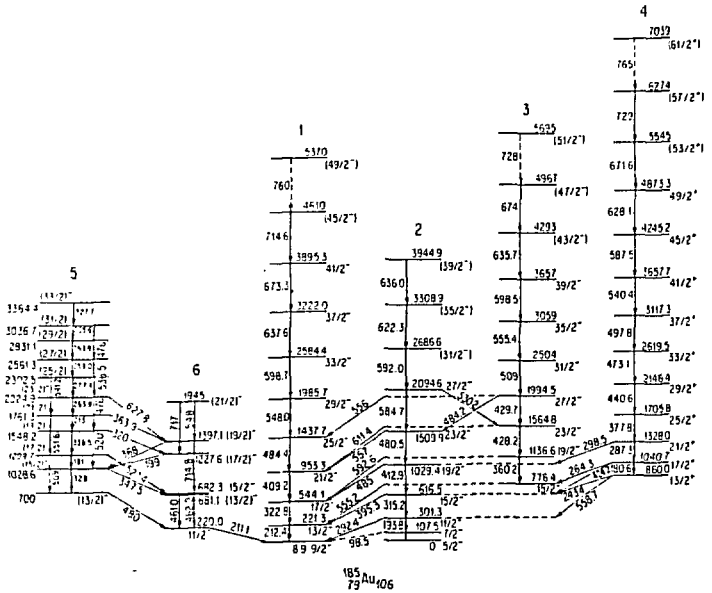

Fig. 1. Levels of ^{185}Au populated in (^{19}F,4n) measurements at McMaster University [3].

As discussed above, bands 1 through 4 in ^{185}Au are thought to be built on prolate Nilsson states. We find that the $h_{9/2}$ bands (1 and 2) have different band crossing features than the $\pi i_{13/2}$ band 4, which in turn reflects the pattern exhibited by the yrast band of the core nucleus, ^{184}Pt. These band crossing features are shown in Fig. 2 via plots of aligned angular momentum versus rotational frequency. The values of I_x and $\hbar\omega$ are extracted from the observed spins and transition energies of the bands in the standard way [12]. The aligned angular momentum , i, is then $I_x - R$, where R is the rotational angular momentum and is approximated by the Harris formula, $(\mathcal{J}_0 + \mathcal{J}_1\omega^2)\omega$. The values of the Harris parameters are

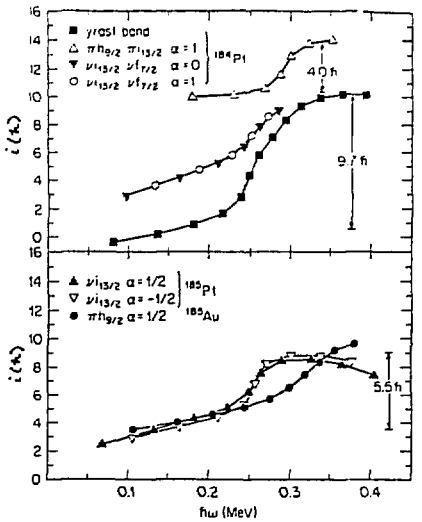

Fig. 2. Aligned angular momentum (i) in units of ħ versus rotational frequency for selected bands in ^{184,185}Pt and ^{185}Au. The alignment gains in the band crossings are shown. The Harris parameters used for all bands are $\mathcal{J}_0$ = 22 MeV^{-1} and $\mathcal{J}_1$ = 110 MeV^{-3}.

shown for each i vs. ħω plot.

The two primary fingerprints of a band crossing are the frequency of the crossing and the alignment gain. As seen in Fig. 2, the yrast band of ^{184}Pt shows a crossing at ħω = .28 MeV with a gain in i of 9.7 ħ. Although the blocking arguments between ^{185}Au and ^{184}Pt suggested the interpretation that this crossing results from the alignment of $\pi h_{9/2}$ [4], subsequent calculations suggested a $\nu i_{13/2}$ crossing [13]. Now our much more complete data on the various nuclei in this region demonstrate that both of these alignment processes occur in the range of 0.26 to 0.29 MeV in frequency. When blocking the ^{184}Pt core with $\nu i_{13/2}$ in the 9/2[624] band of ^{185}Pt, one still observes a crossing, but with a Δi = 5.5 ħ.

When blocking the ^{184}Pt core with $\pi h_{9/2}$ in the 1/2[541] band of ^{185}Au, one still observes a crossing, once again with about half of the total alignment gain. This pattern can only be explained by the occurrence of both $\pi h_{9/2}$ and $\nu i_{13/2}$ crossings at nearly degenerate frequencies, each with an alignment gain of around 5 $\hbar$. Furthermore, there is a self-contained blocking comparison in ^{184}Pt, where two side bands are observed and have been drawn on the alignment diagram of Fig. 2 [14]. One band is thought to be $\pi h_{9/2}\pi i_{13/2}$ in nature, and shows a crossing with $\Delta I = 4$ $\hbar$. The other side band is built on the long-lived isomer observed by Beshai et al. [15], is assigned as $\nu i_{13/2}\nu f_{7/2}$, and has a crossing of similar alignment gain. Once again, one needs to assign two crossings to explain this pattern.

A verification of this "double-crossing" scenario for the yrast band of ^{184}Pt comes from a "double-blocking" measurement in ^{186}Au, where high-spin states are observed for the first time in our work [16]. Some of the bands deduced in ^{186}Au are analogous to those built on the isomeric 11^- states in the heavier odd-odd Au isotopes (A = 190 to 194) [17]. These bands were explained [17] as resulting from the $\pi h_{11/2}\nu i_{13/2}$ coupling in an oblate shape minimum. However, in ^{186}Au the yrast band is strongly coupled and associated with the $\pi h_{9/2}\nu i_{13/2}$ coupling; another band is seen and assigned $\pi h_{9/2}\nu f_{7/2}$. It is logical that these two structures have become yrast, since we see in the odd-A Au isotopes that the $\pi h_{9/2}$ single-particle state falls rapidly in energy and becomes the ground state at A = 185. The high-spin properties of these two prolate bands in ^{186}Au are shown in Fig. 3. It is clear that the former band exhibits no band crossings up to a frequency of 0.4 MeV, reasonable since both the $\pi h_{9/2}$ and $\nu i_{13/2}$ crossings are blocked. The latter band has a single crossing, judging by the gain in i, which is logical since only the $\pi h_{9/2}$ crossing is blocked here. This pattern of bands in ^{185,186}Au and ^{184,185}Pt thus demonstrates the nearly degenerate proton and neutron band crossings. This is the first known example of the "first backbend" really being two alignment crossings.

There are two curious features concerning these two band

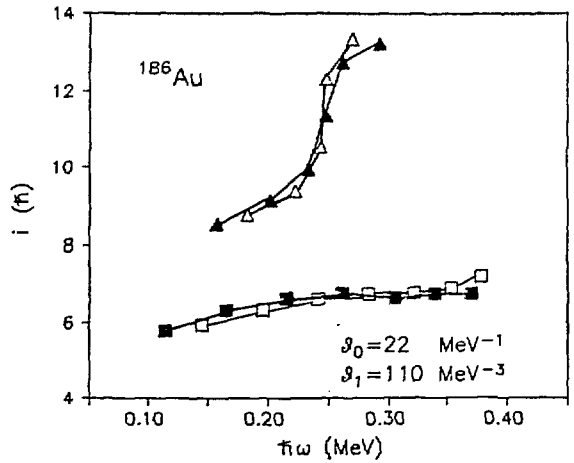

Fig. 3. Alignment versus frequency for the $\pi h_{9/2}\nu i_{13/2}$ (squares) and the $\pi h_{9/2}\nu f_{7/2}$ (triangles) bands in ^{186}Au.

crossings. The first is that their frequencies are quite similar, since there is no other known case where the $\pi h_{9/2}$ crossing occurs as early as the $\nu i_{13/2}$ backbend. The second curious fact is that the alignment gain in the $\nu i_{13/2}$ crossing is only approximately 5 $\hbar$, about one half of the value one expects for this crossing in general. These two features are illustrated in Fig. 4, which gives the alignment diagram for the yrast bands of N = 106 isotones of Os, Ir, and Pt. The ^{182}Os ground band, measured by Lieder et al. [18], exhibits a first backbend which appears to be due to $\nu i_{13/2}$ alignment based on blocking arguments. The frequency of this crossing is similar to that seen for ^{184}Pt, but the alignment gain in Os is approximately 10 $\hbar$. The proton crossing is not observed in ^{182}Os, but is thought to be at a high frequency since Lieder et al. [19] observe it at $\hbar\omega = 0.40$ MeV in ^{180}Os. In ^{183}Ir, the yrast band (1/2[541]) was first measured up to I = 41/2 by Andre et al. [20],

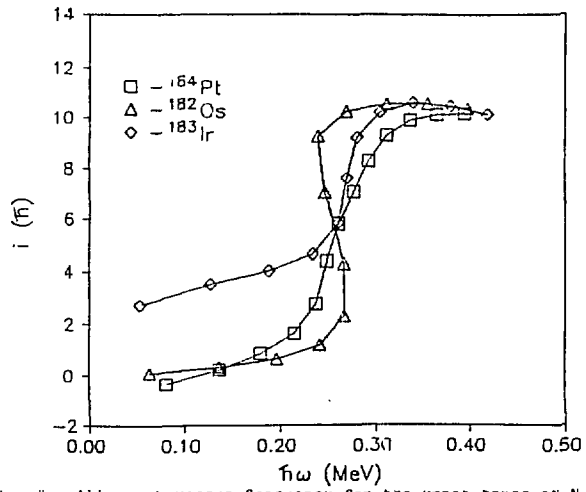

Fig. 4. Alignment versus frequency for the yrast bands of N = 106 isotones of Os [18], Ir, and Pt. The Harris parameters used are $\mathcal{J}_0, \mathcal{J}_1$ = (22,110) for Pt, (23,80) for Ir, and (24,70) for Os.

and now extended to 53/2 by our McMaster measurement. Note that the $\nu i_{13/2}$ crossing occurs in the $\pi h_{9/2}$ band in ^{183}Ir at a similar frequency to the Os isotone, but the Δi has dropped to 6.5 ħ. This then gives rise to a smooth decrease in alignment gain for the $\nu i_{13/2}$ crossing since we conclude from the blocking arguments that this Δi in ^{184}Pt is around 5 ħ.

Although it is difficult to conclude precise crossing frequencies in ^{184}Pt when the two are so close, one can make good estimates from the side bands or from bands in adjacent odd-A nuclei. As illustrated in Fig. 2, one can estimate that the $\pi h_{9/2}$ crossing occurs at ħω = 0.26 MeV, the $\nu i_{13/2}$ at ~ 0.29 MeV. In order to follow the trend of these two alignment processes to other nuclei in this region, we have performed measurements on the N = 104 cases ^{183}Au and ^{182}Pt. No rotational bands had been previously observed in the former, while the yrast band of the latter had been known up to I = 12 [21]. The results are shown in the alignment diagram of Fig. 5. Similar to ^{185}Au, the 1/2[541] and 1/2[660] bands are observed in ^{183}Au. The crossings present in these two bands are different, as is the case in ^{185}Au [3]. The $\pi i_{13/2}$

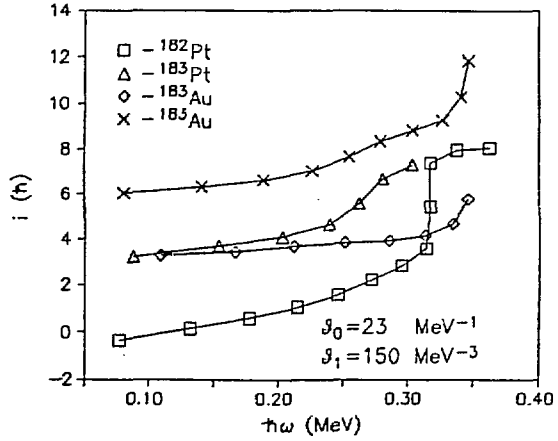

Fig. 5. Alignment versus frequency for bands in ^{182,183}Pt and ^{183}Au. The crosses refer to the $\pi i_{13/2}$ band, the diamonds to the $\pi h_{9/2}$ band, the triangles to the $\nu i_{13/2}$ band.

band shows crossings at ħω = 0.27 and 0.34 MeV, while the $\pi h_{9/2}$ band shows only the latter. The former crossing is apparent in our results on the $\nu i_{13/2}$ band in ^{183}Pt, while the latter cannot be judged since the results do not extend to high enough spins. It is likely that both crossings are present in the core nucleus ^{182}Pt, although the first is difficult to judge since it is rather dependent on the choice of reference parameters. We have used reference parameters which vary smoothly across this N = 104 to 108

and Z = 76 to 79 region, so we are confident of the presence of two crossings in ^{182}Pt. From the pattern of crossings in the various bands in Fig. 5, it is clear that the $\pi h_{9/2}$ crossing occurs at $\hbar\omega$ = 0.47 MeV, the $\nu i_{13/2}$ at ~ 0.33. The neutron crossing thus moves as a function of N, whereas the proton crossing does not.

Our measurements of bands in various nuclei in this region give rise to the systematic trends for the $\nu i_{13/2}$ and the $\pi h_{9/2}$ crossings shown in Fig. 6. Concerning the former, the trend is very similar

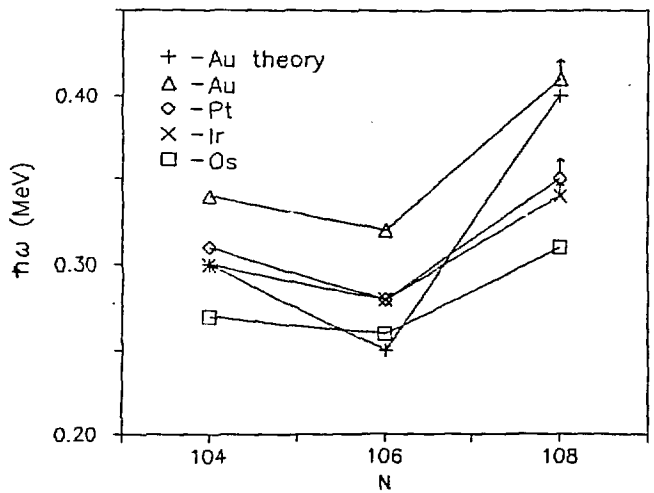

Fig. 6. Systematics of the $\nu i_{13/2}$ crossing frequency versus N for isotopes of Os, Ir, Pt, and Au. The frequencies deduced from the calculations of Zhang et al. [22] are also shown.

for isotopes of Os through Au, viz. the $\nu i_{13/2}$ crossing drops slightly in frequency from N = 104 to 106 and then rises steeply for 108. The experimental trend for the latter is that the $\pi h_{9/2}$ crossing is very high in frequency for Os nuclei, but drops rapidly for Pt and Au. The question is whether these two trends can be understood in terms of some logical variation in the shape parameters in this transition region. Zhang has led a large set of self-consistent calculations of the potential-energy surfaces in this region [22] and has reported on them at this conference. The shape parameters (β_2, β_4, and γ) are calculated in a self-consistent manner as a function of N, Z, $\hbar\omega$, and quasiparticle configuration using a Woods-Saxon potential. Within the limits of the mesh size of the calculations (0.05 MeV in frequency), the crossing frequency between different bands can be deduced from the calculations. These calculated crossing frequencies are also shown in Fig. 6. The experimental trend for $\nu i_{13/2}$ is very nicely reproduced by the calculations, lending some experimental verification to the theoretical values. The values of the deformation parameters for ^{183,185,187}Au, given in the figure caption, are the values immediately before the $\nu i_{13/2}$ crossing. Of course, this quasiparticle alignment process changes the deformation of the nucleus, driving β_2 to a smaller value and γ more negative.

The trend of the measured $\pi h_{9/2}$ crossing is shown in Fig. 7 as a function of Z for various values of N. This proton crossing is at a high frequency for Os nuclei, but then drops rapidly for Pt and Au. A comparison with calculated values of the crossing frequency is shown in Fig. 7, although the theoretical values are extracted in a different manner than for those in Fig. 6. The proton crossing does occur at a rather high frequency for Os nuclei in the calculations, in fact beyond the grid of the self-consistent calculations. We therefore must resort to using the self-consistent shape parameters after the $\nu i_{13/2}$ crossing in a normal Cranked Shell Model calculation, one which uses a Woods-Saxon potential and a smooth decrease in proton pairing just like that used in the self-consistent calculations. The resulting theoretical crossing frequencies are seen in Fig. 7 to be significantly higher than the measured values, although the trend is correct.

In conclusion, our measurements have demonstrated for the first

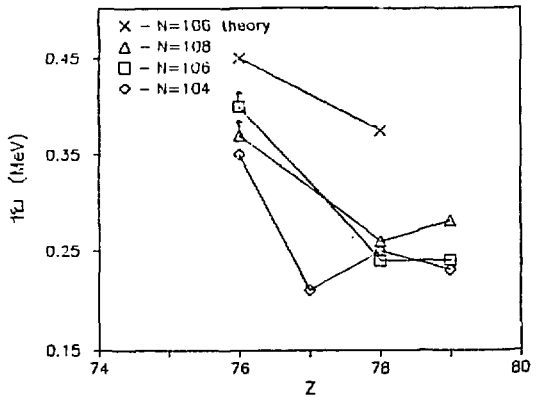

Fig. 7. Trend of $\pi h_{9/2}$ crossing frequency versus Z for N = 104, 106, and 108. The calculated values are shown for 106; these assume (β_2, β_4, γ) values of (0.225,-0.041,-2°) for Os and (0.230,-0.027,-2°) for Pt.

time the occurrence of low-lying $\nu i_{13/2}$ and $\pi h_{9/2}$ band crossings in the N ~ 106 region of prolate, oblate, and spherical shapes. The truly transitional nature of this region is demonstrated by the co-existence of bands built on prolate and oblate states in ^{185}Au (our in-beam results), and by transitions with enhanced E0 components between states of equal spins coupled to the $h_{9/2}$ and $h_{11/2}$ shell states (UNISOR measurements [8]). This variation of the nuclear shape with respect to N, Z, and configuration is also reflected in the fact that the crossing frequencies for the neutron and proton alignment processes change rather markedly across this region. Initial comparisons with the self-consistent calculations of the potential-energy surfaces [22] indicate that the shape parameters deduced can explain many of the measured features. We then appear to be close to having the first detailed roadmap of the way the nuclear shape changes from the strong prolate values of the rare-earth region to the spherical parameters expected for lead isotopes.

This work is supported by the US Department of Energy under contract No. DE-AS05-76ER0-4936. The assistance of technical staff at the Oak Ridge and McMaster accelerator facilities is gratefully acknowledged. Discussions with and calculations from J.-Y. Zhang have been crucial in this project.

References

[1] J.-y. Zhang et al., Phys. Rev. C28 (1983) 446.
[2] L.L. Riedinger et al., ACS symposium on "Recent Advances on the Study of Nuclei off the Line of Stability", Chicago, 1985.
[3] A.J. Larabee et al., Phys. Lett. 169B (1986) 21.
[4] A.C. Kahler et al., Phys. Lett. 72B (1978) 443.
[5] M.G. Desthuilliers et al., Nucl. Phys. A313 (1979) 221.
[6] V. Berg et al., Nucl. Phys. A410 (1983) 445.
[7] W. Nazarewicz, to be published.
[8] M. Kortelahti et al., Bull. Am. Phys. Soc. 31 (1986) 874.
[9] J.L. Wood, in Proc. 4th International Conf. on Nuclei far from Stability, Helsingor, CERN Report 81-09 (1981) 612.
[10] U. Garg et al, ACS symposium on "Recent Advances on the Study of Nuclei off the Line of Stability", Chicago, 1985.
[11] J.H. Hamilton et al, Phys. Rev. Lett. 35 (1975) 562.
[12] For example, L.L. Riedinger, Nucl. Phys. A347 (1980) 141.
[13] S. Frauendorf et al., in Future Directions in Studies of Nuclei Far From Stability, North-Holland, New York (1980) 133.
[14] M.P. Carpenter et al., to be published.
[15] S.Beshai et al., Z. Phys. A277 (1976) 351.
[16] Z.-m. Liu et al., to be published.
[17] A. Neskakis et al., Nucl. Phys. A390 (1982) 53.
[18] R.M. Lieder et al., Nucl. Phys. A375 (1982) 291.
[19] R.M. Lieder et al., Nucl. Phys. to be published.
[20] S. Andre et al., Phys. Rev. Lett. 38 (1977) 327.
[21] C.M. Lederer and V.S. Shirley, Table of Isotopes, J. Wiley & Sons, New York (1978).
[22] R. Bengtsson, G. Leander, W. Nazarewicz, and J.Y. Zhang, to be published.

Accepted for publication in Nuclear Instruments and Methods.

STUDIES OF NUCLEAR ROTATIONAL BANDS WITH THE SPIN SPECTROMETER

L.L. RIEDINGER, M.P. CARPENTER, L.H. COURTNEY, and V.P. JANZEN
Department of Physics, University of Tennessee, Knoxville, TN 37996, USA

In the last few years increasingly sophisticated gamma-ray spectrometer arrays have been built at a number of laboratories around the world. These instruments, coupled with versatile heavy-ion accelerators, are capable of probing the detailed behaviour of atomic nuclei under extreme conditions of angular momentum and temperature. Characteristics of one such detector array, the Spin Spectrometer at Oak Ridge National Laboratory, are presented here. Representative gamma-ray data are shown, illustrating the practical differences that result from using two unlike accelerator beams to produce the same nucleus. Finally, the application of the data to the question of quasiparticle rotational alignment in light Pt and Au nuclei is discussed.

1. Introduction

A number of technical developments in recent years have given great impetus to the study of nuclei at high angular momentum. Heavy-ion accelerators have been able to produce the variety of beams needed to form nuclear reaction products at high spins, and the ever improving arrays of gamma-ray counters have enabled the study of the emissions from states in these rapidly rotating nuclei. These new techniques have given rise to a real explosion in the knowledge of many nuclei in the range of 20 to 40 $\hbar$ of angular momentum, with recent examples of rotational bands of levels being observed in the $I > 40\ \hbar$ region. From this vast amount of experimental data, much has been learned about the sharing of angular momentum between rotational and single-particle modes in yrast and near-yrast excitations of the nucleus. This is the physics of rather cold but very rapidly rotating nuclei that is being learned through the high-spin spectroscopy of discrete gamma-ray lines emitted following the heavy-ion reaction.

The heavy-ion reaction product is usually left in a state of high energy and high angular momentum, which decays by the emission of a long sequence of (20 to 30) gamma rays to the ground state. The multi-element arrays of gamma-ray counters are essential for the efficient study of these high multiplicity gamma-ray events. There are 4π detector arrays at a number of heavy-ion accelerators in the world, each differing somewhat in the number and nature of the elements. The purpose of this paper is to describe one type of nuclear

high-spin study that is now possible with the Spin Spectrometer at the Holifield Heavy Ion Research Facility (HHIRF) at the Oak Ridge National Laboratory. This array of NaI detectors (71 when composed only of this type) is now being used in conjunction with up to 18 Compton-suppressed Ge counters for a variety of measurements at the HHIRF. Twelve of these annular suppressors are made of bismuth germanate (BGO), and an additional ten units made of NaI are available. This Compton-suppression system has been described by Johnson et al. [1], while the Spin Spectrometer specifications have been discussed by Jaaskelainen et al. [2].

In this paper, the use of this instrumentation in the study of high-spin states in ^{184}Pt is described. This is a transitional nucleus, one on the border between the region of well-deformed nuclei (Sm through Os) and those of near-spherical shapes closer to the Pb closed shell. In such a transitional nucleus, one encounters deformed shapes that are quite susceptible to the deforming influences of the single-particle orbits with large individual angular momenta. It is the influence of these high-j quasiparticles on the soft core that we study in this transitional region. Similar studies are much more complete in mapping the incidence of deformation at the beginning of the rare-earth deformed region [3].

2. Technique

High-spin states have been studied in ^{184}Pt by two reactions. At the HHIRF, the ^{154}Sm(^{34}S,4n) reaction was used with a beam energy of 163 MeV incident on two 0.5 mg/cm^2 targets. Seven Ge detectors were placed at various angles in the Spin Spectrometer, leaving 64 NaI counters. Six of these Ge counters were surrounded by annular NaI Compton suppression units. The full system of 18 Compton-suppressed Ge counters had not been fully implemented when these measurements were performed. A second measurement was performed at the McMaster University Tandem Accelerator using the ^{172}Yb(^{16}O,4n) reaction at an energy of 91 MeV and a lead-backed target. The spectroscopy data were collected with an array of eight Ge and six NaI counters. In addition, an angular distribution experiment involving five Ge detectors placed at various angles to the beam direction was performed at McMaster, in order to deduce the